ISSN print: 1224-5984
ISSN online: 2248-3942

Rom Biotechnol Lett. 2021; 26(6): 3155-3165
doi: 10.25083/rbl/26.6/3155-3165

Received for publication, February, 23, 2021
Accepted, April, 13, 2021

Original paper

Regulation of the intestinal dysbiosis of high – fat diet obese mice via gut microbia–TLR$_{2/4}$ pathway by electroacupuncture

YUAN–CHENG SI[1], CHEN–CHEN REN[1], BO CHEN[1], QING–QING LI[1], WEI–JUN DING[2]

[1] Academy of Acupuncture and Tuina , Guizhou University of Traditional Chinese Medicine, Dongqing South Road, Guiyang, 550025 P. R. China.
[2] Department of Fundamental Medicine, Chengdu University of Traditional Chinese Medicine, Liutai Road 1166, Wenjiang District, Chengdu, 610037 P. R. China.

Abstract

Objective: We design experimental study to explore the impacts of electroacupuncture (EA) treatment on the interaction between TLR$_{2/4}$ pathway and gut flora in high – fat diet obese mice.
Methods: Reverse transcriptase polymerase chain reaction, western blotting and 16S rRNA pyrosequencing were to study the association among groups (normal (N), model (M), electroacupuncture for 7 d (A7), 14 d (A14), 21 d (A21) and 28 d (A28) group).
Results: EA reduced the relative expression of TLR$_{2/4}$ gene and protein, and regulated the significant difference species flora in different levels, such as *Firmicutes* and *Actinobacteria* in Phylum, *Coriobacteriia* in Class, *Coriobacteriales* in Order, *Atopobiaceae* in Family, and *Oscillibacter*, I*ntestinimonas*, *Lachniclostridium* and *Acetatifactor* in Genus. In all acupuncture groups, the analytical data of A21 group was similar to normal mice.
Conclusion: These findings suggested the interaction between TLR$_{2/4}$ pathway and gut flora could be a novel target of EA treatment against obesity.

Keywords Electroacupuncture; Obesity; TLR$_{2/4}$; Intestinal flora; 16S rRNA pyrosequencing.

To cite this article: SI YC, REN CC, CHEN B, LI QQ, DING WJ. Regulation of the intestinal dysbiosis of high – fat diet obese mice via gut microbia–TLR$_{2/4}$ pathway by electroacupuncture. *Rom Biotechnol Lett*. 2021; 26(6): 3155-3165. DOI: 10.25083/rbl/26.6/3155-3165.

*Corresponding author: YUAN–CHENG SI, Academy of Acupuncture and Tuina, Guizhou University of Traditional Chinese Medicine, Dongqing South Road, Guiyang, 550025 P. R. China. Tel: (+86) 0851 8830 8024, Fax: (+86) 0851 8830 8024.
E-mail: siyuancheng039@gzy.edu.cn

Introduction

Obesity has become an increasing and serious chronic disease. According to the updated WHO statistics, there are approximately 1.9 billion overweight people in the world, of which 600 million meet the obesity standard (Wang, 2019). The obesity status in China is still grim, the adult overweight rate is as high as 31.5 %, and the obesity rate reaches 12.2 % (Tian, 2019). Obesity is a high–risk factor that can cause or worsen diseases of hypertension, diabetes, hyperlipidemia and cancers (Hersoug, 2018; Ding, 2009). So, a multitude of researchers commit to investigate the underlying mechanisms of obesity. A great number of studies of obesity have focused on energy metabolic disorders and low level of inflammatory (Henao–Mejia, 2012). Recently, the imbalance of gut flora is attracting extensive attentions (Boulangé, 2016). Accumulated publications show that the formation of obesity is closely related to the intestinal dysbiosis (Si, 2018). The dysbiotic intestinal flora of obesity patients or animal models have been repeatedly displayed along with the progress of obesity (Chassaing, 2015).

Toll–like receptors (TLRs) recognize a variety of pathogen-associated molecular patterns and induce innate immune responses (O'Neill, 2008). They connect innate immunity to adaptive immune responses between human beings and gut flora. Among TLRs, TLR_4 detects lipopolysaccharides (LPS) found in most gram–negative bacteria (Jang, 2017), whereas TLR_2 recognizes lipopeptides and other components of gram– positive bacteria (Caricilli, 2011). Moreover, TLR_2 and TLR_4 are intensively associated with inflammatory cytokines (Ji, 2019). The expression of TLR_2 and TLR_4 in intestinal tissues are markedly increased in obese and overweight patients (Jialal, 2014).

Acupuncture as a green and non–drug therapy has been successfully used to resolve a series of diseases, such as gastrointestinal, functional and painful diseases (Belivani, 2013). It is also as an effective method applied to lose weight (Cho, 2009) for millions of people worldwide (Firouzjaei, 2016). Theoretically, acupuncture can modulate the interrelationships of intestinal chronic inflammatory response and gut flora though meridian system (Liang, 2014; Brahma, 2016). However, few studies have been conducted on the regulation mechanisms of acupuncture between chronic inflammation and gut flora. Therefore, we hypothesized that electroacupucture (EA), one of the common approaches of acupuncture (Yuan, 2016), could regulate the cross–talking of gut microbia-$TLR_{2/4}$ pathway to achieve the purpose of weight–loss. Thus, we examined in the present work the hypothesis by a high-fat diet (HFD) induced obese mice model.

Materials and Methods

Animals and groups

The Animal Ethics Committee of Guizhou University of Traditional Chinese Medicine (TCM) approved this study. C57BL/6 mice in SPF criterion (aged 8 weeks and weight 19.58 ± 1.49 g at the beginning of the experiment) were purchased from SPF (Beijing) Biotechnology Co., Ltd. (Certificate number: SCXK (Jing) 2016-0002), every six mice were raised in a plastic cage. Mice were fed in an environment-controlled lab (23℃–25℃, 50%–70% humidity) with a 12/12–light/dark cycle with *ad libitum* access to tap water and diet.

Obesity mice were established by HFD (composition: 60 kcal% fat, 20 kcal% carbohydrate, 20 kcal% protein; 5.24 kcal/g total energy content, H10060) from Beijing Huakangkang Biotechnology Co., Ltd. (Rivera, 2015). 30 obesity mice were obtained after HFD for 8 weeks; their weights were 20% more than the normal (N). Then, these obesity mice were randomly divided into obesity model (M), electroacupuncture for 7 d (A7), 14 d (A14), 21 d (A21) and 28 d (A28) group.

EA treatment

Animals of the EA groups were given EA treatment at the points of Tianshu (ST25), Guanyuan (CV4), Zusanli (ST36) and Zhongwan (CV12) (Yin, 2008). Acupuncture needles (0.18 × 30 mm) were inserted into ST25, CV4, ST36 and CV12 to a depth 3 mm, approximately. In order to achieve "deqi", or local tissue fibrillation, we applied the needle twisting method and connected to a G6805-III electrostimulator (Suzhou Medical Supplies Co., Ltd., China) with an intensity of 2–3 mA and a frequency of 30 Hz for 10 min (Zhang, 2012). Such intensity was maintained just below the level that induced visible muscle contraction. EA were performed daily, alternatively at the left or right side of these points. Mice of the normal and model groups were fixed 10 min in the same way without EA.

Lee's index detection

All mice were weighted per week by an electronic scale (range: 0–200 g, definition: 0.01 g) and measured body lengths weekly by a soft ruler (range:0–100 cm, definition: 0.2 cm). Then, the Lee's index was calculated as: (Lee's index= (weight (g) * 1000) ^ 1/3 / length (cm).

Extraction of serum and intestinal tissue

The serum and intestinal tissues were collected at 7^{th}, 14^{th}, 21^{th} and 28^{th} day after EA treatment. The blood samples were collected form femoral artery, and the serum were taken after rest the blood for 30 min and centrifugation at 3000 g for 10 min. These blood samples were stored at –80℃ for further biochemical tests. The subjects were sacrificed by cervical dislocation, the small intestinal tissues including the peyer's patch were homogenized and centrifuged, and 400 μL of the supernatant was taken in an EP tube and stored at –80 ℃ for subsequent analysis.

Enzyme -linked immunosorbent assay

Six mice in each group were ramdomly selected for Enzymelinked immunosorbent assay measurement. Refer to the manufacturer's instructions of the kits (Genetimes ExCell Technology Company, China), the levels of IL_{-6}, $IL_{-1\beta}$ and $TNF_{-\alpha}$ were measured carefully in the serum and supernatants. Absolute quantification of intestinal inflammatory factors in intestinal tissue samples were analyzed by Milliplex (ELX808IUP, USA BioTek).

Western blotting

The homogenate of the small intestine was splitted with a lysis buffer, containing a cocktail of phosphatase and proteinase inhibitors and PMSF (Chauhan, 2019). Following denaturation, the lysates were separated on a 10% SDS–PAGE gel and transferred to polyvinylidene difluoride PVDF membranes. The membranes blocked with 5% non–fat powdered milk in TBST (Tris-HCl buffered saline (PH8.8) containing 0.1% Tween20) for 1 h at room temperature and then incubated overnight at 4℃ with a monoclonal rabbit anti–TLR$_4$ (1: 1000, Proteintech Group), anti–TLR$_2$ (1: 1000, Proteintech Group), or anti–GAPDH (1: 5000, Proteintech Group) primary antibody. After washing in TBST, the membrane was incubated for 1 h at RT with a HRP–conjugated goat anti–rabbit antibody (1:1000; Jackson Immunoresearch Laboratories, PA, USA), and the protein bands were visualized using Enhanced Chemiluminescence Kit (Thermo, Production batch: PICPI23223). Images of the protein bands were recorded using the Image Quant LAS 4000 system (Tanon-5200, Tanon, USA), and the band intensities were quantified using Imagequant TL software (version 2.2.4, Tanon, USA). The density of proteins was quantified by Quantity One (Thermo, USA). Three mice in each group were randomly selected for Western blotting.

16S rRNA pyrosequencing

The cecum content of each mouse was sterilely collected and saved in –80℃ refrigerator. Total genome DNA was extracted and separated using Cetyl Trimethyl Ammenium Bromide and SDS method (Avershina, 2013). The concentration and purity of DNA samples were monitored on 1% agarose gel and adjusted to 1ng μL $^{-1}$ using sterile water. The V3 and V4 regions of 16S rRNA gene were amplified to use specific primers with the barcode (Larsson, 2012). All PCR reactions were carried out with High-Fidelity PCR Master Mix (New England Biolabs). Mixed the same volume of 1× loading buffer (contained SYB green) with PCR products and operated electrophoresis on 2% agarose gel. Samples with bright main strip between 400–450 bp were chosen for further experiments. Then, mixture PCR products were purified with Qiagen Gel Extraction Kit (Qiagen, Germany). Sequencing libraries were generated using DNA PCR–Free Sample Preparation Kit (Illumina, USA) following manufacturer's recommendations. The library quality was assessed on the 2.0 Fluorometer (Thermo Scientific) and Agilent Bioanalyzer 2100 system (Walker, 2015; Huse, 2012). At last, the library was sequenced on an Illumina HiSeq 2500 platform.

Bioinformatics analysis

Raw data of the 16S rRNA pyrosequencing was continuously split, assembled, filtrated and the chimera was removed (Edgar, 2013). Then using a uparse software to analyze the sequences data of operational taxonomic units (OTUs) production which sequences with 97% similarity were assigned to the same OTUs. Representative sequence for each OTU was screened for further annotation. Ribosomal database project 3 classifier conducted a further analysis on the basis to draw OTUs cluster and Species annotation (Version 2.2) (Stegen, 2016). Calculated with QIIME and displayed with R Software (Version 2.15.3) (Lundberg, 2013; Caporaso, 2010) to apply in analyzing complexity of species diversity for samples. Statistical tests on the taxonomic differences among samples were calculated by Welch's t–test combined with Welch's inverted method for calculating confidence intervals (nominal coverage of 95%), using the statistical analysis of metagenomic profiles software version 2.0 (Lundberg, 2013).

Statistical analysis

SPSS Software (V22.0; SPSS Inc., Chicago, IL) was used for statistical analyses. All experiment data were indicated as the Means ± Standard Deviation. Data were analyzed with one-way ANOVA. Differences between the groups were evaluated using Student–Newman–Keuls. Data were considered to be significantly different with each value of $^{*}p < 0.05$, $^{**}p < 0.01$.

Results and discussion

EA improved obesity index of HFD mice

To observe the effects of EA on treating obese mice, some fundamental parameters were constructed. The body weight and length in experiment period were measured. Repeated measurements ANOVA of fundamental data showed no significant effects of body weight and Lee's index before EA treatment among obese mice. However, there were significant differences of weight (Figure 1a, F value = 23.21, $p< 0.01$) and Lee's index (Figure 1b, F value= 9.59, $p < 0.01$) after EA treatment between model group and acupuncture groups. These results indicated that EA intervention could reduce weight and Lee's index indicators.

EA reduced the level of inflammation in intestinal tissue

To evaluate whether EA treatment could regulate the levels of proinflammatory cytokines, the IL$_{-1\beta}$ (Figure 1c), IL$_{-6}$ (Figure 1d) and TNF$_{-\alpha}$ (Figure 1e) in intestinal tissue had been measured. Data analysis showed that the content of IL$_{-1\beta}$ in M group was significantly lower than N group (F value =11.44，$p < 0.01$), but the content of IL$_{-6}$ (F value = 19.58, $p < 0.01$) and TNF$_{-\alpha}$ (F value = 14.52, $p <$ 0.01) in M group were significantly higher than N group. Then, the content of IL$_{-1\beta}$ was improved significantly and the content of IL$_{-6}$ and TNF$_{-\alpha}$ were reduced significantly after EA treatment. In addition, the parameter indexes in IL$_{-6}$ and IL$_{-1\beta}$ in A21 group were changed significantly among acupuncture groups ($p< 0.05$). These results demonstrated that EA intervention could regulate the levels of proinflammatory cytokines in intestinal tissue of obese mice.

EA decreased the expression of TLR$_{2/4}$ in intestinal tissue

To research whether EA treatment could mediate TLR$_{2/4}$ pathways to mitigate intestinal inflammatory response. The protein distribution density of TLR$_2$ (Figure 2a) and TLR$_4$ (Figure 3a) in intestinal tissue were detected by

immunehistochemical method. Additionally, the positive expression rate in TLR_2 (Figure 2b, F value = 5.68, $p < 0.01$) and TLR_4 (Figure 3b, F value = 7.42, $p < 0.01$) of M group was significantly higher than N group and reduced significantly after EA intervention. Moreover, we measured relative expression of genes (Figure 2c, F value = 6.37, $p < 0.01$; Figure 3c, F value = 17.59, $p < 0.01$) and proteins (Figure 2d, F value = 13.26, $p < 0.01$; Figure 3d, F value = 8.22, $p < 0.01$) in TLR_2 and TLR_4 of M group were significantly higher than N group. Furthermore, the relative expression of genes and protein were significantly lower in acupuncture groups. The mice of A21 group ($p < 0.05$) were changed significantly among acupuncture groups. Therefore, these results showed that EA intervention could mediate $TLR_{2/4}$ pathways to alleviate intestinal inflammatory response.

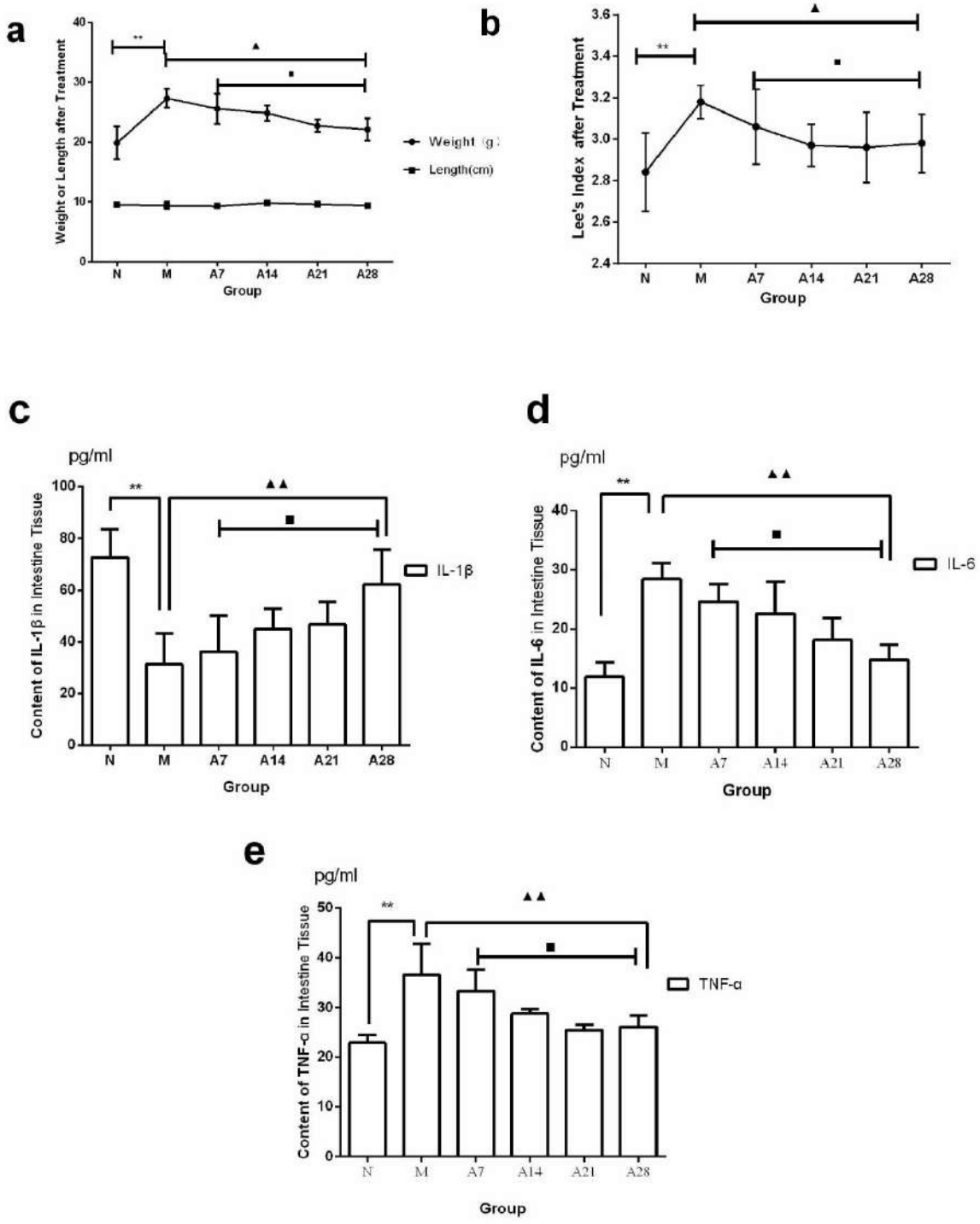

Figure 1

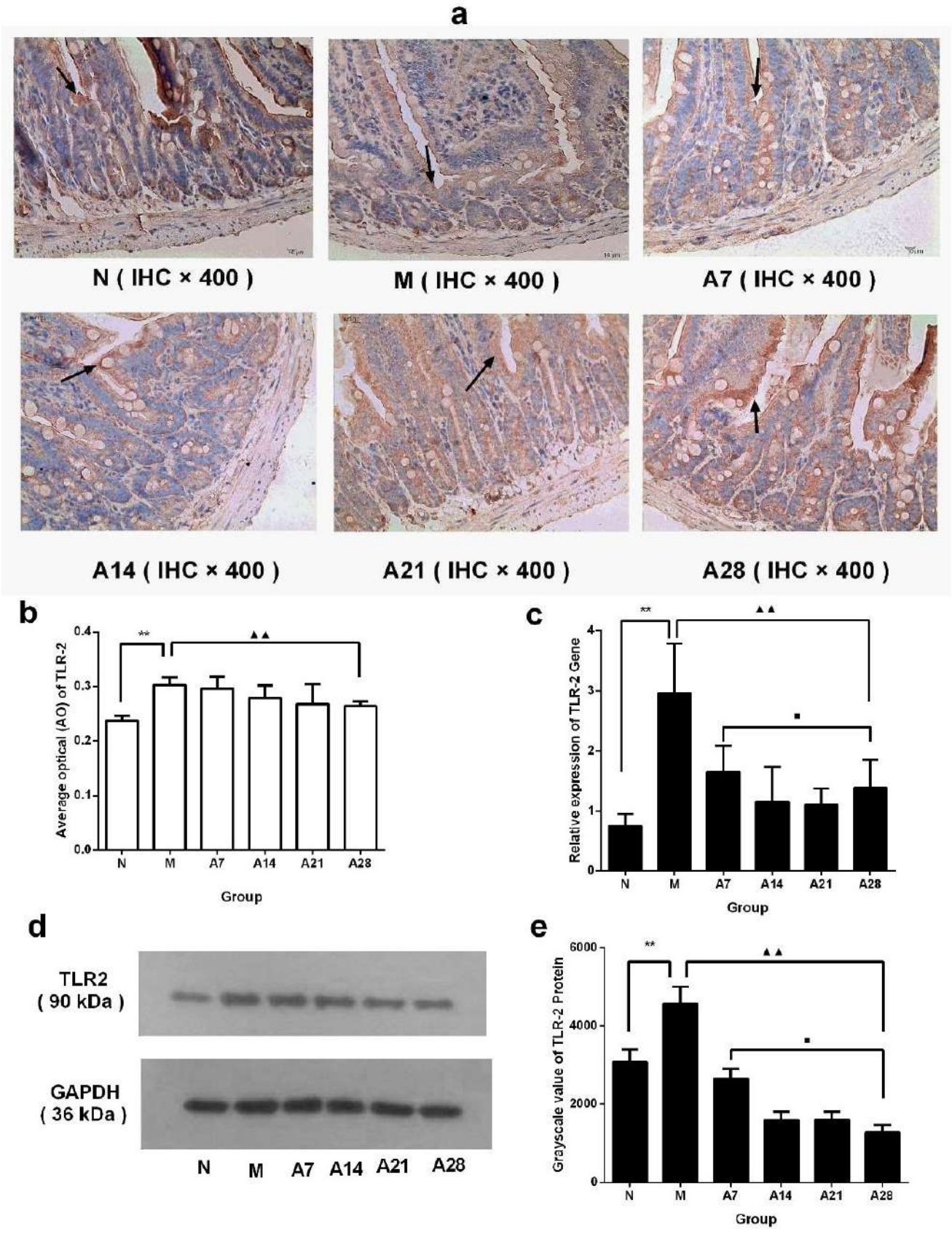
a
N (IHC × 400)
M (IHC × 400)
A7 (IHC × 400)
A14 (IHC × 400)
A21 (IHC × 400)
A28 (IHC × 400)
b
Average optical (AO) of TLR-2
0.0
0.1
0.2
0.3
0.4
**
▲▲
N
M
A7
A14
A21
A28
Group
c
Relative expression of TLR-2 Gene
0
1
2
3
4
**
▲▲
▪
N
M
A7
A14
A21
A28
Group
d
TLR2
(90 kDa)
GAPDH
(36 kDa)
N
M
A7
A14
A21
A28
e
Grayscale value of TLR-2 Protein
0
2000
4000
6000
**
▲▲
▪
N
M
A7
A14
A21
A28
Group

Figure 2

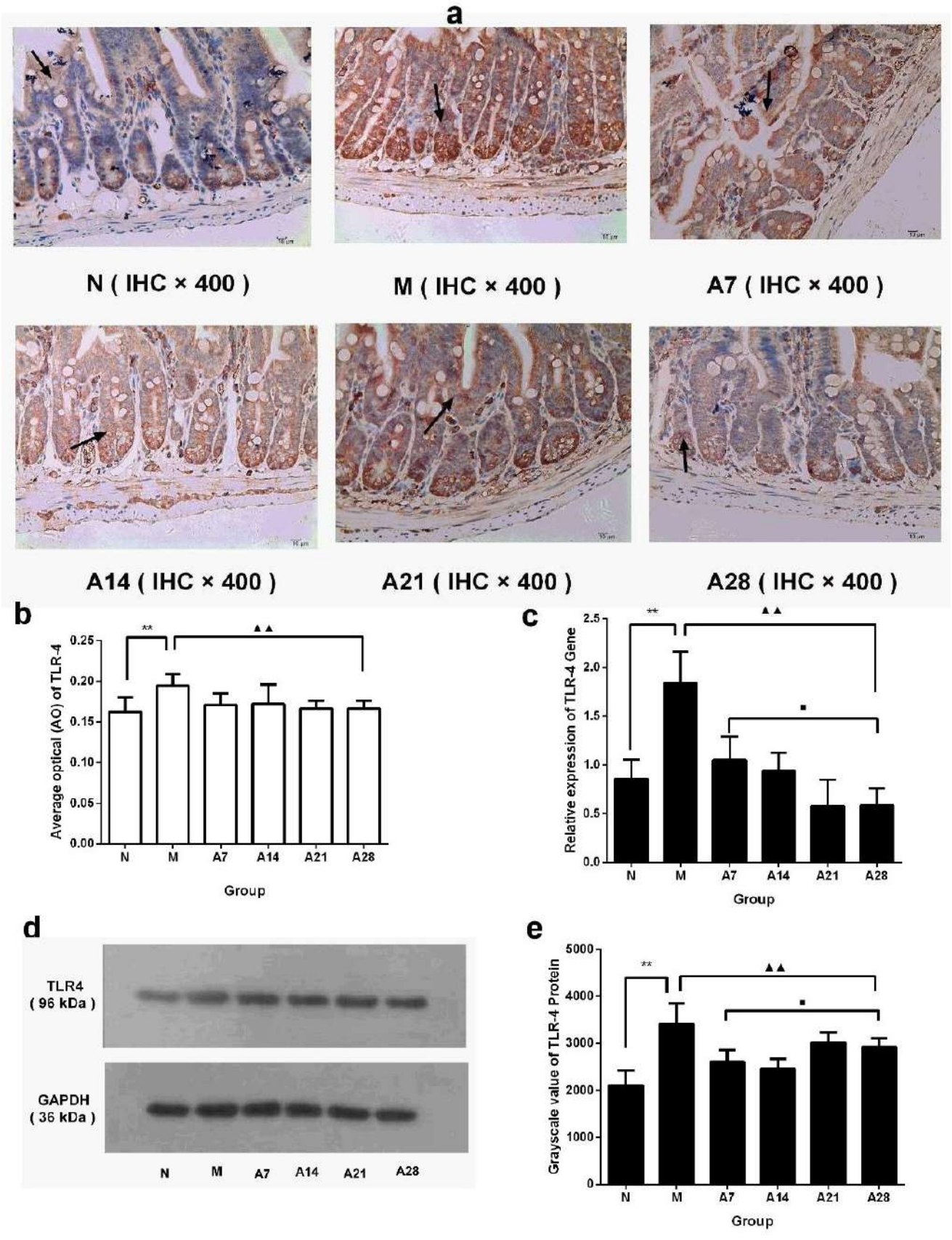
a
N (IHC × 400)
M (IHC × 400)
A7 (IHC × 400)
A14 (IHC × 400)
A21 (IHC × 400)
A28 (IHC × 400)
b
Average optical (AO) of TLR-4
0.25
0.20
0.15
0.10
0.05
0.00
**
▲▲
N
M
A7
A14
A21
A28
Group
c
Relative expression of TLR-4 Gene
2.5
2.0
1.5
1.0
0.5
0.0
**
▲▲
*
N
M
A7
A14
A21
A28
Group
d
TLR4
(96 kDa)
GAPDH
(36 kDa)
N
M
A7
A14
A21
A28
e
Grayscale value of TLR-4 Protein
5000
4000
3000
2000
1000
0
**
▲▲
*
N
M
A7
A14
A21
A28
Group

Figure 3

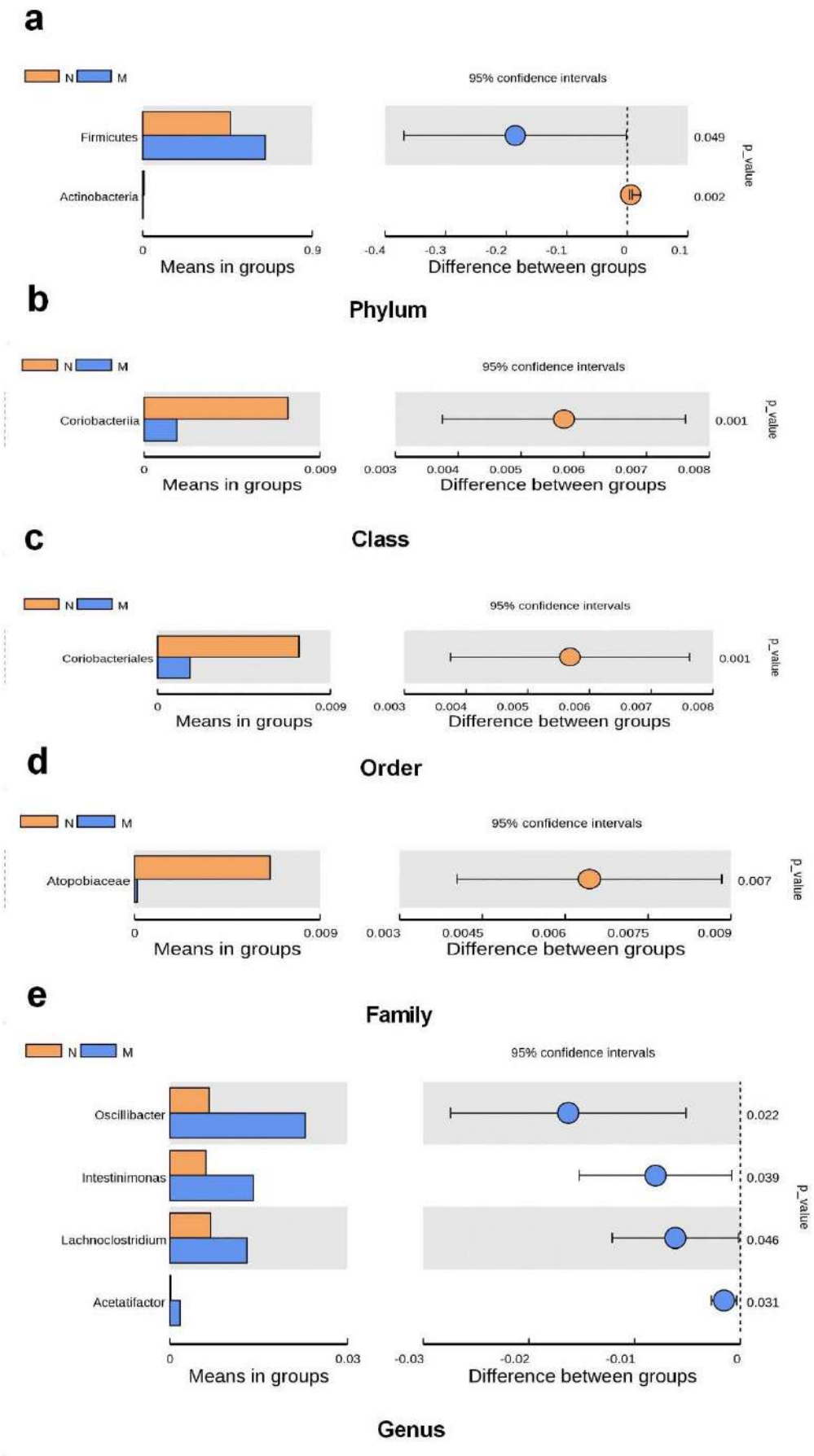
a
N M
95% confidence intervals
Firmicutes
Actinobacteria
0.049
0.002
p_value
0
0.9
Means in groups
-0.4
-0.3
-0.2
-0.1
0
0.1
Difference between groups
b
Phylum
N M
95% confidence intervals
Coriobacteriia
0.001
p_value
0
0.009
Means in groups
0.003
0.004
0.005
0.006
0.007
0.008
Difference between groups
c
Class
N M
95% confidence intervals
Coriobacteriales
0.001
p_value
0
0.009
Means in groups
0.003
0.004
0.005
0.006
0.007
0.008
Difference between groups
d
Order
N M
95% confidence intervals
Atopobiaceae
0.007
p_value
0
0.009
Means in groups
0.003
0.0045
0.006
0.0075
0.009
Difference between groups
e
Family
N M
95% confidence intervals
Oscillibacter
Intestinimonas
Lachnoclostridium
Acetatifactor
0.022
0.039
0.046
0.031
p_value
0
0.03
Means in groups
-0.03
-0.02
-0.01
0
Difference between groups
Genus

Figure 4

EA restored the intestinal microbial diversity dysbiosis in obese mice

In this study, we measured intestinal microbial diversity by Illumina next- generation sequencing technology to observe the regulatory effect of EA treatment on the intestinal flora. The intestinal microbial diversity results showed that there were significant difference of cecal flora in different level, such as *Firmicutes* (Figure 4a, p= 0.049) and *Actinobacteria* (Figure 4a, p= 0.002) in Phylum level, *Coriobacteriia* (Figure 4b, p= 0.001) in Class level, *Coriobacteriales* (Figure 4c, p = 0.001) in Order level, *Atopobiaceae* (Figure 4d, p= 0.007) in Family level, and *Oscillibacter* (Figure 4e, p = 0.022), *Intestinimonas* (Figure 4e, p = 0.039), *Lachniclostridium* (Figure 4e, p = 0.046)and *Acetatifactor* (Figure 4e, p = 0.031) in Genus level (Figure 4e, p = 0.022). In beta diversity analysis of gut flora composition, the bacterial species in the cecal microbial diversity in M group mice were significantly lower than N group, but the bacterial species were significantly higher after EA treatment (Figure 5a, F value = 12.78, p< 0.01). The A28 group were changed significantly among acupuncture groups. As showed in Figure 5b, principal component analysis of samples across all groups further demonstrated that EA treatment regulated the community composition of obese mice to normal (F value = 14.26, p < 0.01). The Figure 5c data was showed directly that the community composition of A21 group was most similar to that of the N group (F value= 7.53, p < 0.01). Thence, EA intervention might regulate intestinal microbial diversity dysbiosis in obese mice to reach losing weight.

In the present study, our team had proved that EA treatment could regulate gut flora dysbiosis in obese mice (Si, 2018). EA treatment could tune the compositions and metabolic functions of gut flora of obese mice to normal conditions. It was from the balance between gut flora and host metabolism to research the pathogenesis of obesity.

In this study, we focused on the mechanism of action between intestinal flora and chronic inflammation of the intestines. In addition, we presented inspiring result: obese mice could be losing weight with EA by stimulating the ST25, CV4, ST36 and CV12 points. A meta–analysis of acupuncture acupoints and simple obesity showed that these acupoints were applied more frequently (Fang, 2017). The body weight and Lee's index were designed as fundamental indicators to evaluate effect of losing weight by acupuncture (Hou, 2015). We established a HFD induced obese model (Yin, 2008) with acupuncture intervention for 7 d, 14 d, 21 d, and 28 d. Afterwards, compared with obese mice, the results of which showed significant difference in fundamental indicators of acupuncture groups (Figure 1). These displayed that EA could have effect of losing weight on the overall level.

In further in-depth research, the level of proinflammatory cytokines in $IL_{-1\beta}$, IL_{-6} and $TNF_{-\alpha}$ of intestinal peyer' patch was significantly abnormal compared to the normal mice. Intestinal peyer' patch were a crucial immune tissue in the intestine and rich in more than 80% of the intestinal cells (Bak, 2010). Simultaneously, these were also a paramount organization for monitoring and regulating intestinal flora (Clarke, 2012). As showed in Figure 1 e–g, the content of $IL_{-1\beta}$ in intestinal peyer' patch of obese mice was lower significant, but the content of IL_{-6} and $TNF_{-\alpha}$ were higher. Moreover, the proinflammatory cytokines of $IL_{-1\beta}$, IL_{-6} and $TNF_{-\alpha}$ were an important active substance to activate the intestinal mucosa immune response and trigger the $TLR_{2/4}$ signaling pathway (Zhang, 2019). $TLR_{2/4}$ pathway was a key to link and transduce intestinal flora and immunity (Larsson, 2012). On the one hand, a quintessential example should be cited that TLR_4 identified exogenous pathogens by binding to LPSs of GNB and induced the non-specific immune responses in the macrophage to product antimicrobial peptides mediating the function and structure of the intestinal flora (Velloso, 2015). On the other hand, LPS bound to TLR_4 and induced a $NF_{-\kappa B}$ dependent inflammatory cascade resulting in excessive production of $TNF_{-\alpha}$ and IL_{-6}. These proinflammatory cytokines were initially beneficial in bacterial killing, but eventually damaged the host's cells and tissues. The positive expression rate and relative expression of genes and proteins in $TLR_{2/4}$ with obese mice were significantly higher than normal mice (Figure 2, Figure 3). However, a series of parameters of $TLR_{2/4}$ such as protein distribution density, the relative expression of gene and protein were reduced significantly after EA treatment. In different acupuncture groups, A21 group was better than others.

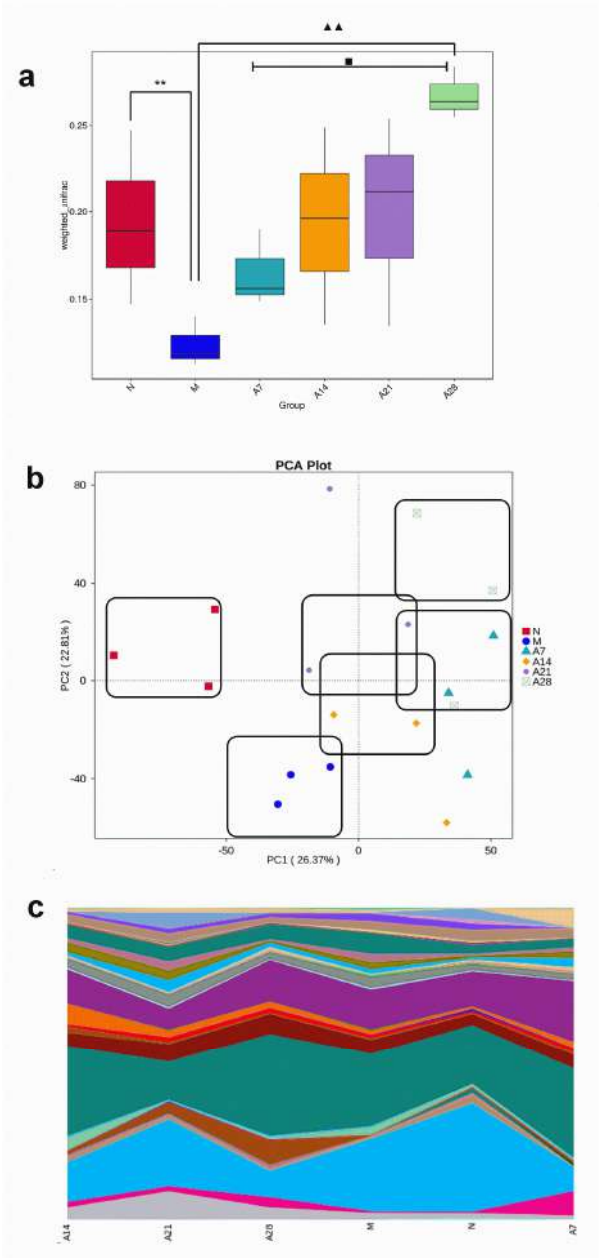

Figure 5

16S rRNA sequencing is the main method for studying the difference in microbial diversity (Caporaso, 2010). 16S rRNA sequencing is the use of conserved regions on the 16S rRNA of the small ribosomal subunit of prokaryotic cells to identify the genetic relationship among the bacteria, and further analyze the significant differences in α diversity and β diversity (Fabbiano, 2018). In the study of in-depth obesity, the research group used the latest technology to explore the effective ways of obesity and treatment. Moreover, we discovered significant differences in five level (Phylum, Class, Order, Family and Genus), such as *Firmicutes, Actinobacteria, Coriobacteriia, Coriobacteriales, Atopobiaceae, Oscillibacter, Intestinimonas, Lachniclostridium* and *Acetatifactor* (Figure 4). *Firmicutes, Actinobacteria, Coriobacteriales* and *Intestinimonas* were all belonged to GPB, which cell wall contained peptidoglycan, pectic acid and mucopolysaccharide (Yatsunenko, 2012). These ingredients could activate the intestinal mucosal immune response via the TLR_2 pathway. Additionally, the other significant difference bacterial were rich in LPSs of cell wall. The LPSs could bind to TLR_4 for transferring intestinal mucosal immune response (Avershina, 2013). After EA treatment, the structural composition of the intestinal flora was regulated significantly. Especially, the data of A21 group was similar to normal mice (Figure 5c).

This study investigated the interaction between $TLR_{2/4}$ pathway and gut flora in obese mice was impacted by EA for the first time. Previous studies of losing weight mechanisms of EA were majorly focused on the regulation in BMI, body fat, WHR or neuroendocrine modulation (Yin, 2008; Hou, 2015). $TLR_{2/4}$ pathway had used to study inflammatory metabolic reactions in the past. Few researchers combined $TLR_{2\ /\ 4}$ pathways with intestinal flora to study obesity-related problem. Therefore, we were first to report the interaction between $TLR_{2/\ 4}$ pathway and intestinal flora. These finds suggest that might be considered as a novel target for EA treatment.

Results indicated that could be used to determine the correlation between EA and the change in gut microbia–$TLR_{2/4}$ pathway, particularly screening out the significant difference species of different levels that were a target of EA therapy against obesity. Our primary study was to some extent short of samples, especially in confronting such a complex disease as obesity. Notwithstanding its limitation, this study implied that the interaction was a key to lose weight by EA. Furthermore, an in – depth study was needed to confirm the above findings and to evaluate the underlying mechanisms between $TLR_{2/\ 4}$ pathway and intestinal flora by EA.

Conclusion

In summary, the present work demonstrated a novel weight-loss approach of EA regulating the gut flora dysbiosis based on restoring the gut microbia–$TLR_{2/4}$ pathway in obese mice to normal conditions. In addition, we provided an evidence of an impotent crosstalk between $TLR_{2/4}$ and intestinal flora. This pathophysiological link might be one of the reasonable explanations for obesity.

Conflicts of Interest

The authors declare that they have no conflicts of interest.

Acknowledgments

This work was supported by the National Natural Science Foundation of China (No. 81860775; No. 81273899); Guizhou Education Department Youth Science and Technology Talents Growth Project (CN) (No. Qian – Jiao – He KY (2018) 219).

References

1. Avershina E, Frisli T, Rudi K. De novo semi–alignment of 16S rRNA gene sequences for deep phylogenetic characterization of next generation sequencing data. *Microbes Environ.* 2013; 28: 211 – 216. doi: 10.1264/jsme2.me12157
2. Bak EJ, Park HG, Kim JM, Yoo YJ, et al. Inhibitory effect of evodiamine alone and in combination with rosiglitazone on in vitro adipocyte differentiation and in vivo obesity related to diabetes. *Int. J. Obes (Lond).* 2010; 34: 250–260. doi: 10.1038/ijo.2009.223
3. Belivani M, Dimitroula C, Katsiki N, Apostolopoulou M, et al. Acupuncture in the treatmentof obesity: A narrative review of the literature. *Acupunct Med.* 2013; 31: 88–97. doi: 10.1136/acupmed-2012- 010247
4. Boulangé CL, Neves AL, Chilloux J, Nicholson JK, et al. Impact of the gut microbiota on inflammation, obesity, and metabolic disease. *Genome Med.* 2016; 8(1): 42. doi: 10.1186/s13073-016-0303-2.
5. Brahma Naidu P, Uddandrao VV, Ravindar Naik R, Suresh P, et al. Ameliorative potential of gingerol: promising modulation of inflammatory factors and lipid marker enzymes expressions in HFD induced obesity in rats. *Mol Cell Endocrinol.* 2016; 419:139–147. doi: 10.1016/j.mce.2015. 10.007.
6. Caporaso JG, Kuczynski J, Stombaugh J, Bittinger K, et al. QIIME allows analysis of high – throughput community sequencing data. *Nat Methods.* 2010; 7: 335–336. doi: 10.1038/nmeth.f.303
7. Caricilli AM, Picardi PK, de Abreu LL, Ueno M, et al. Gut microbiota Is a key modulator of insulin resistance in TLR 2 knockout mice. *PLoS Biol.* 2011; 9(12): e1001212. doi: 10.1371/journal.pbio. 1001212.
8. Chassaing B, Koren O, Goodrich JK, Poole AC, et al. Dietary emulsifiers impact the mouse gut microbiota promoting colitis and metabolic syndrome. *Nature.* 2015; 519 (7541): 92–96. doi: 10.1038/nature14232

9. Chauhan A, Pandey N, Desai A, Raithatha N, et al. Association of TLR4 and TLR9 gene polymorphisms and haplotypes with cervicitis Susceptibility. *PLoS One.* 2019; 14: e0220330. doi: 10.1371/journal. pone.0220330
10. Cho SH, Lee JS, Thabane L, Lee J. Acupuncture for obesity: A systematic review and meta-analysis. *Int J Obes (Lond).* 2009; 33: 183–196. doi: 10.1038/ijo.2008.269
11. Clarke SF, Murphy EF, Nilaweera K, Ross PR, et al. The gut microbiota and its relationship to diet and obesity: new insights. *Gut Microbes.* 2012; 3: 186–202. doi: 10.4161/gmic.20168
12. Ding WJ, Deng Y, Feng H, Liu WW, et al. Biotransformation of aesculin by human gut bacteria and identification of its metabolites in raturine. *World J Gastroenterol.* 2009;15(12):1518–1523. doi：10.3748/wjg.15.1518
13. Edgar RC. UPARSE: highly accurate OTU sequences from microbial amplicon reads. *Nat Methods.* 2013; 10: 996–998. doi: 10.1038/nmeth.2604
14. Fabbiano S, Suárez–Zamorano N, Chevalier C, Lazarević V, et al. Functional gut microbiota remodeling contributes to the caloric restriction-induced metabolic improvements. *Cell Metab.* 2018; 28: 907–921. doi: 10.1016/j.cmet.2018.08.005
15. Fang S, Wang M, Zheng Y, Zhou S, et al. Acupuncture and lifestyle modification treatment for obesity: A meta-analysis. *Am J Chin Med.*2017; 45(2):239−254. doi: 10.1142/S0192415X1750015X
16. Firouzjaei A, Li GC, Wang N, Liu WX, et al. Comparative evaluation of the therapeutic effect of metformin monotherapy with metformin and acupuncture combined therapy on weight loss and insulin sensitivity in diabetic patients. *Nutr Diabetes.* 2016;6: e209. doi: 10.1038/nutd.2016.16
17. Henao-Mejia J, Elinav E, Jin C, Hao L, et al. Inflammasome-mediated dysbiosis regulates progression of NAFLD and obesity. *Nature.* 2012; 482(7384): 179–185. doi：10.1038/nature10809
18. Hersoug LG, Møller GP, Loft S. Role of microbiota−derived lipopolysaccharide in adipose tissue inflammation, adipocyte size and pyroptosis during obesity. *Nutr Res Rev.* 2018; 31(2):153–163. doi：10.1017/S0954422417000269
19. Hou PW, Hsu HC, Lin YW, Tang NY, et al. The history, mechanism, and clinical application of auricular therapy in traditional Chinese medicine. *Evid Based Complement Alternat Med.* 2015; 2015: 495684. doi: 10.1155/2015/495684
20. Huse SM, Ye Y, Zhou Y, Fodor AA. A core human microbiome as viewed through 16S r RNA sequence clusters. *PLoS One.* 2012; 7: e34242. doi: 10.1371/journal.pone.0034242
21. Jang JC, Li J, Gambini L, Batugedara HM, et al. Human resistin protects against endotoxic shock by blocking LPS-TLR4 interaction. *Proc Natl Acad Sci USA.* 2017; 114(48): E10399–E10408. doi: 10.1073/pnas.1716015114
22. Ji Y, Sun S, Shrestha N, Darragh LB, et al. Toll-like receptors TLR2 and TLR4 block the replication of pancreatic β cells in diet−induced obesity. *Nat Immunol.* 2019; 20: 677–686. doi: 10.1038/ s41590-019-0396-z
23. Jialal I, Kaur H, Devaraj S. Toll-like receptor status in obesity and metabolic syndrome: a translational perspective. *J Clin Endocrinol Metab*. 2014; 9: 39–48. doi: 10.1210/jc.2013-3092
24. Larsson E, Tremaroli V, Lee YS, Koren O, et al. Analysis of gut microbial regulation of host gene expression along the length of the gut and regulation of gut microbial ecology through MyD88. *Gut.* 2012; 61:1124–1131. doi: 10.1136/gutjnl-2011-301104
25. Liang Y, Gong D. Acupuncture for chronic pelvic inflammatory disease: A qualitative study of patients' insistence on treatment. *BMC Complement Altern Med.* 2014; 14: 345. doi: 10.1186/1472-6882-14- 345
26. Lundberg DS, Yourstone S, Mieczkowski P, Jones CD, et al. Practical innovations for high-throughput amplicon sequencing. Nat Methods. 2013; 10: 999–1002. doi: 10.1038/nmeth.2634
27. O'Neill LA. The interleukin-1 receptor/Toll-like receptor superfamily: 10 years of progress. *Immunol Rev.* 2008; 226:10–18. doi: 10.1111/j.1600-065X.2008.00701.x
28. Rivera HM, Kievit P, Kirigiti MA, Bauman LA, et al. Maternal high−fat diet and obesity impact palatable food intake and dopamine signaling in nonhuman primate offspring. *Obesity (Silver Spring).* 2015; 23: 2157–2164. doi: 10.1002/oby.21306
29. Si YC, Miao WN, He JY, Chen L, et al. Regulating gut flora dysbiosis in obese mice by electroacupuncture. Am J Chin Med. 2018; 46:1481–497. DOI: 10.1142/S0192415X18500763
30. Stegen JC, Hurlbert AH, Bond-Lamberty B, Chen X, et al. Aligning the measurement of microbial diversity with macroecological theory. *Front Microbiol.* 2016; 7: 1487. doi: 10.3389/fmicb.2016. 01487
31. Tian S, Liu Y, Xu Y, Feng A. Does obesity modify the epidemiological association between hyperuricemia and the prevalence of hypertension among Northern Chinese community- dwelling people? A Chinese population-based study. *BMJ Open.* 2019; 9(11): e031803. doi：10.1136/ bmjopen-2019-031803
32. Velloso LA, Folli F, Saad MJ. TLR4 at the crossroads of nutrients, gut microbiota and metabolic inflammation. *Endocr Rev.* 2015; 36: 245–271. doi: 10.1210/er.2014-1100
33. Walker AW, Martin JC, Scott P, Parkhill J, et al. 16S rRNA gene−based profiling of the human infant gut microbiota is strongly influenced by sample

processing and PCR primer choice. *Microbiome.* 2015; 3: 26. doi: 10.1186/s40168-015-0087-4

34. Wang Y, Hooper LV. Immune control of the microbiota prevents obesity. *Science.* 2019; 365(6451): 316–317. doi：10.1126/science. aay 2057
35. Yatsunenko T, Rey FE, Manary MJ, Trehan I, et al. Human gut microbiome viewed across age and geography. *Nature.* 2012; 486: 222–227. doi: 10.1038/nature11053
36. Yin CS, Jeong HS, Park HJ, Baik Y, et al. A proposed transpositional acupoint system in a mouse and rat model. *Res Vet Sci.* 2008; 84: 159–165. doi: 10.1016/j.rvsc.2007.04.004.
37. Yuan M, Li Y, Wang Y, Zhang N, et al. Electroacupuncture at ST37 enhances jejunal motility via excitation of the parasympathetic system in rats and mice. *Evid Based Complement Alternat Med.* 2016; 2016: 3840230. doi: 10.1155/2016/ 3840230
38. Zhang J, Diao B, Lin X, Xu j, et al. TLR2 and TLR4 mediate an activation of adipose tissue renin-angiotensin system induced by uric acid. *Biochimie.* 2019; 162:125–133. doi: 10.1016/ j.biochi. 2019.04.013
39. Zhang ZJ, Wang XM, McAlonan GM. Neural acupuncture unit: A new concept for interpreting effects and mechanisms of acupuncture. *Evid Based Complement Alternat Med.* 2012; 2012: 429412. doi: 10.1155/2012/429412